Development 130, 3715-3724

doi:10.1242/dev.00602

Echinoid limits R8 photoreceptor specification by inhibiting inappropriate EGF receptor signalling within R8 equivalence groups

Emma L. Rawlins, Neil M. White and Andrew P. Jarman*

Wellcome Trust Centre for Cell Biology, Institute of Cell and Molecular Biology, University of Edinburgh, King's Buildings, Edinburgh EH9 3JR, UK

*Author for correspondence (e-mail: andrew.jarman@ed.ac.uk)

Accepted 14 May 2003

SUMMARY

EGF receptor signalling plays diverse inductive roles during development. To achieve this, its activity must be carefully regulated in a variety of ways to control the time, pattern, intensity and duration of signalling. We show that the cell surface protein Echinoid is required to moderate Egfr signalling during R8 photoreceptor selection by the proneural gene *atonal* during *Drosophila* eye development. In *echinoid* mutants, Egfr signalling is increased during R8 formation, and this causes isolated R8 cells to be replaced by groups of two or three cells. This mutant phenotype resembles the normal inductive function of Egfr in other developmental contexts, particularly during *atonal*-controlled neural recruitment of chordotonal sense organ precursors. We suggest that *echinoid* acts to prevent a similar inductive outcome of Egfr signalling during R8 selection.

Key words: EGF receptor, *Drosophila*, Photoreceptor, R8

INTRODUCTION

The control of widely deployed signalling pathways is a central issue of developmental cell biology. This is true of Epidermal Growth Factor Receptor (Egfr) signalling, which plays diverse roles during *Drosophila melanogaster* eye development (e.g. Freeman, 1996; Dominguez et al., 1998; Chen and Chien, 1999; Baonza et al., 2001). Often these different roles seem spatially and temporally to be overlapping, raising questions of how distinct cellular responses are regulated. This report concerns the regulation of Egfr signalling during the selection of R8 photoreceptors.

The patterning of the *Drosophila* compound eye as a hexagonal array of ommatidia depends on precise spacing of the ommatidia, which in turn relies on selection and patterning of founding R8 photoreceptor cells in a regular grid within the undifferentiated retinal ectoderm. This requires complex cell interactions that are incompletely understood, but involve an interplay between cell signalling and the proneural gene *atonal* (*ato*). *ato* encodes a bHLH transcription factor that endows cells with R8 competence. R8 patterning is a progressive process and this is reflected in the evolution of the Ato expression pattern. In the eye imaginal disc, Ato is initially expressed in a stripe of cells just anterior to the morphogenetic furrow as it traverses the unpatterned ectoderm (Jarman et al., 1994). As the wave of expression moves on, the stripe becomes broken into evenly spaced clusters of cells, with Ato expression inhibited between them. Each of these 'intermediate groups' (IGs) is analogous to the proneural clusters of bristle SOPs (Jarman et al., 1995). Within each IG, Ato expression is then resolved to a solitary R8 precursor before being completely downregulated (Dokucu et al., 1996).

Complex cellular interactions regulate *ato* during IG patterning and R8 selection. The regular interruption of *ato* expression that gives rise to a nascent row of IGs depends on inhibitory signalling from the previous row of spaced IGs. Mutations in genes involved in this process result in irregular and denser IG spacing, as is seen for the secreted molecule Scabrous (Sca) (Ellis et al., 1994). A number of studies have implicated Egfr/Raf/Ras signalling in IG spacing, possibly in cooperation with Notch (Dominguez et al., 1998; Spencer et al., 1998; Chen and Chien, 1999; Baonza et al., 2001), although this conclusion is not universally accepted (Kumar et al., 1998).

R8 selection within the IGs is a separate event from IG patterning, although the two are often confused because some genes are required in both processes, including *Notch* and *sca* (Baker et al., 1996). In principle, R8 selection is akin to sense organ precursor (SOP) formation (e.g. for sensory bristles) in that it involves Notch-mediated lateral inhibition within groups of competent cells defined by *ato* expression (the IGs being equivalent to SOP proneural clusters). Nevertheless, there is evidence for at least two discrete steps in the refinement process that reveals unexpected (and unaccounted for) complexity. The first step is the refinement of Ato expression and R8 competence to a group of three cells distinguished initially by virtue of their raised nuclei (Dokucu et al., 1996) and then by low level expression of the R8 marker encoded by *senseless* (*sens*) (Frankfort et al., 2001). Dokucu and colleagues named this the R8 equivalence group (Dokucu et

al., 1996). The second step is the restriction of R8 fate to one of these three cells, coinciding with restriction of *ato* and *sens* expression. The equivalence group represents a group of cells that are uniquely primed to take on an R8 fate. This is apparent in a number of gene mutations that result in extra R8 cells specifically from the equivalence group rather than the IG as a whole, as observed in *sca* (Ellis et al., 1994) and *rough* (*ro*) mutants, and also after experimental overexpression of *ato* (Dokucu et al., 1996; White and Jarman, 2000). In these mutations, the normally isolated R8 cells are frequently replaced by twins and triplets – the so-called 'R8 twinning' phenotype.

The role of Egfr signalling in R8 selection has been contentious because of contradictory evidence. Most studies have concluded that while Egfr/Raf/Ras signalling may be required for correct IG spacing, such signalling is not absolutely required for a cell to take on an R8 fate (Dominguez et al., 1998; Kumar et al., 1998). For example, R8 selection can occur within Egfr mutant clones, albeit aberrantly (Dominguez et al., 1998). Nevertheless, Egfr signalling appears to be active during R8 selection (Kumar et al., 1998; Wasserman et al., 2000) and other evidence has been presented that suggests Egfr/Raf/Ras signalling is required for R8 fate (Spencer et al., 1998). Thus, R8 selection within the equivalence group is poorly understood.

We recently described the effect of overexpressing *ato* in the developing R8 precursors using an R8 specific *Gal4* driver (*109-68Gal4*) to drive UAS-*ato* (*ato*$^{109\text{-}68}$) (White and Jarman, 2000). Although such overexpression does not alter the expression pattern of *ato* beyond boosting and extending it within R8 cells, *ato*$^{109\text{-}68}$ exhibited several defects in eye development. One of these defects was R8 twinning, indicating failure of R8 resolution within the equivalence group. This is unexpected because overexpressing *ato* in R8 should increase Notch-mediated lateral inhibition, not reduce it. This non-autonomous effect therefore suggests that undefined signalling mechanisms that impinge on R8 resolution are being affected by *ato* misexpression.

To investigate the process of R8 selection further, we used *ato*$^{109\text{-}68}$ as the basis of a screen for genetic modifiers to isolate mutations that affect R8 resolution. We isolated a mutation of *echinoid* (*ed*), recently described as encoding an L1-like cell adhesion molecule (Bai et al., 2001). The *ed* mutation dominantly enhances the R8 twinning defect of *ato*$^{109\text{-}68}$ and, contrary to a previous report, also exhibits severe R8 twinning as a homozygote. Unexpectedly, our investigation of this phenotype revealed strong indications that the R8 twinning results from derepression of Egfr signalling within the R8 equivalence group causing inappropriate inductive interactions between these cells. We suggest that *ed* acts as a novel Egfr antagonist in this context to downregulate Egfr signalling, and thereby modulate the outcome of signalling.

MATERIALS AND METHODS

Fly stocks

ed$^{4.12}$, *ed*$^{4.4}$ and *ed*$^{6.1}$ were created by EMS mutagenesis (this work). The following alleles have been described previously: *argos*$^{\Delta 3}$ (Freeman et al., 1992); *ed*^{lH23} (de Belle et al., 1993); *l(2)k01102* (Bai et al., 2001); *ato*^{2} (White and Jarman, 2000); *ro*^{X63} (Heberlein and Rubin, 1991); *sca*^{BP2} (Mlodzik et al., 1990); *spi*^{SC2} (Tio et al., 1994). *N*^{55e11} and *Egfr*^{IK35} have been described by Lindsley and Zimm (Lindsley and Zimm, 1992). The R7 enhancer trap was 70-9 (obtained from M. Mlodzik). The Gal4 and UAS lines used were *109-68-Gal4, UAS-ato* (White and Jarman, 2000), *sca-Gal4* (Baker et al., 1996), *GMR-Gal4* (Freeman, 1996), *UAS-sSpi* (Freeman, 1996), *UAS-pntP1* (Klaes et al., 1994) and *UAS-raf*^{ACT} (Scholz et al., 1997). The aberrations used were *Df(2L)ed-dp*, *Df(2L)ed1*, *Dp(2:1)B19* (Lindsley and Zimm, 1992). Fly stocks were maintained on standard cornmeal-yeast-agar medium. Crosses to *UAS-ed* were performed at 29°C to increase Gal4-activity. All other crosses were performed at 25°C.

Mutagenesis

To obtain genetic modifiers of *ato*$^{109\text{-}68}$, male *OrR* flies were fed 25 or 30 mM EMS and then mated to *ato*$^{109\text{-}68}$*/CyO* females. The eyes of the F1 progeny were examined under a dissecting microscope for enhancement or suppression of the rough eye phenotype. Potential modifiers were backcrossed to *ato*$^{109\text{-}68}$*/CyO* and the eyes of the F2 progeny rescored. Further crosses were then performed to determine genetic linkage and establish a balanced stock. Similarly, to obtain further *ed* alleles, male *OrR* flies were fed 25 or 30 mM EMS and then mated to *ed*$^{4.12}$*/CyO* females.

Generation of mitotic clones

Mutant clones were induced using the FLP/FRT method (Xu and Rubin, 1993). *ed* and *spi* clones were marked by the absence of nlsGFP (*2xnlsGFP, FRT40A* flies obtained from A. Gonzalez-Reyes) and induced by *eyelessFLP* (Newsome et al., 2000). Flies had the following genotypes: *y w eyFLP; ed*^{lH23} *FRT40A/2xnlsGFP FRT40A*, *y w eyFLP; ed*$^{4.4}$ *FRT40A/2xnlsGFP FRT40A*, *y w eyFLP; ed*$^{6.1}$ *FRT40A/2xnlsGFP FRT40A*, *y w eyFLP; spi*^{SC2} *FRT40A/2xnlsGFP FRT40A* or *y w eyFLP; ed*$^{4.12}$ *spi*^{SC2} *FRT40A/ed*$^{4.12}$ *2xnlsGFP FRT40A*. *Egfr* clones were induced in a *Minute* background, marked by the absence of β-galactosidase immunoreactivity and created using a heatshock inducible *FLP* (first instar larvae were heat-shocked for 1 hour at 37°C). *Egfr* clones were induced in flies of the following genotypes: *y w hsp70-FLP; FRT42D Egfr*^{IK35}*/FRT42D arm-lacZ M(2)53* (Dominguez et al., 1998), *y w hsp70-FLP; ed*$^{4.12}$ *FRT42D Egfr*^{IK35}*/ed*$^{4.12}$ *FRT42D arm-lacZ M(2)53* or *y w hsp70-FLP; FRT42D Egfr*^{IK35} *sca*^{BP2}*/FRT42D arm-lacZ M(2)53*.

Histology

Scanning electron microscopy (SEM) was performed according to standard procedures and all scanning electron micrographs were taken at 150× magnification on a Cambridge Stereoscan 250. For immunohistochemistry staining, eye-antennal imaginal discs were dissected from wandering third instar larvae and fixed in 3.7% formaldehyde (10-15 minutes). Incubations with primary and secondary antibodies were performed according to standard procedures. Primary antibodies used were affinity purified rabbit anti-Ato (1:2000), mouse anti-Boss (1:200; provided by S. L. Zipursky), guinea-pig anti-Sens (1:5000; provided by H. Bellen), mouse anti-Sca [1:200; Developmental Biology Hybridoma Bank (DBHB), Iowa, USA], mouse anti-Ro (1:200; DBHB), mouse anti E(spl) 323-2-G (1:2; provided by Sarah Bray), rabbit anti-β-galactosidase (1:10000; Cappel) and mouse anti-dpErk (1:500; Sigma). Secondary antibodies (1:1000) were obtained from Jackson Laboratories or Molecular Probes. Confocal fluorescence images were taken on a Leica TCS SP microscope.

For mRNA in situ hybridisation eye-antennal imaginal discs were dissected from wandering third instar larvae, fixed in 3.7% formaldehyde (1 hour) and then dehydrated in ethanol and stored at –20°C until use. DIG-labelled mRNA probes were in vitro transcribed using a DIG RNA labelling kit (Roche). The DIG label was detected using a sheep anti-DIG alkaline phosphatase coupled antibody. Light microscope images were taken on an Olympus AX70 microscope.

RESULTS

Isolation of a mutation in *echinoid* that enhances an activated *ato* phenotype

E(ato$^{109\text{-}68}$)4.12 was isolated as a second site mutation that dominantly enhanced *ato$^{109\text{-}68}$* when present in one copy (Fig. 1B,C). *E(ato$^{109\text{-}68}$)4.12* itself was found to be homozygous viable with a strong rough eye phenotype (Fig. 1D). A lethal allele of *ed* (*ed^{lH23}*) failed to complement *E(ato$^{109\text{-}68}$)4.12*: transheterozygous flies were viable, with rough eyes, suggesting that *E(ato$^{109\text{-}68}$)4.12* is an allele of *ed*. *ed* encodes an L1-like cell adhesion molecule with a novel intracellular domain (Bai et al., 2001). Sequencing the *ed* gene from *E(ato$^{109\text{-}68}$)4.12* homozygotes revealed in the predicted extracellular domain a single amino acid substitution compared with the published Ed protein sequence and with that of the parent line used for the mutagenesis. On the basis of this and other evidence, we therefore renamed this mutation *ed$^{4.12}$*.

R8 photoreceptors are frequently twinned in *ed$^{4.12}$*

Examination of *ed$^{4.12}$/ed$^{4.12}$* eye imaginal discs revealed a very specific defect in the expression pattern of Ato (Fig. 2A-D). In *ed$^{4.12}$* homozygotes Ato expression appeared normal in its initial activation and refinement to IGs, and then R8 equivalence groups. However, there was a severe defect in subsequent refinement of Ato expression within the equivalence groups to single R8 precursors. In a high proportion of equivalence groups, Ato expression remained in two or three cells. To see whether the extra Ato-expressing cells go on to become extra R8 cells, we looked at expression of R8 markers. Sens is activated in R8 precursors as a target of Ato (Frankfort et al., 2001) (Fig. 2A). In *ed* mutants Sens is activated at a similar time to wild type but then remains expressed in the Ato-expressing two or three cell clusters (Fig. 2C). This suggests that all the extra Ato-expressing cells are responding to this expression and behaving as R8 precursors. Boss is a specific marker of differentiating R8s (Van Vactor et al., 1991). In *ed$^{4.12}$*, Boss expression also reveals twinned R8 cells that are relatively evenly spaced (Fig. 2B,D), indicating that some or all of the extra Ato-expressing cells undergo R8 differentiation. This is consistent with the phenotype of multiple R8-like internal photoreceptors seen in adult retinal sections (data not shown). Thus the *ed$^{4.12}$* mutation results in excessive R8 specification from the equivalence groups, i.e. an R8 twinning phenotype.

These findings suggest that *ed$^{4.12}$* is a dominant enhancer of *ato$^{109\text{-}68}$* because it exacerbates the R8 twinning caused by *ato* overexpression. Indeed, we confirmed that *ato$^{109\text{-}68}$*-induced R8 twinning is significantly increased in the presence of one copy of *ed$^{4.12}$* (Table 1). We investigated whether *ed* could also

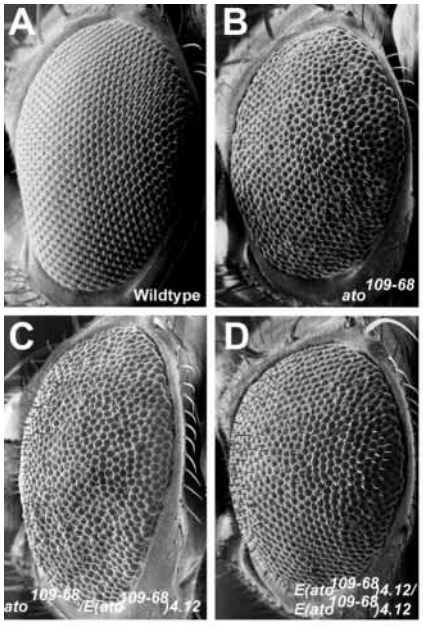

Fig. 1. *E(ato$^{109\text{-}68}$)4.12* enhances the rough eye phenotype of *ato$^{109\text{-}68}$* and also displays a rough eye as a homozygote. (A-D) Scanning electron microscopy of the adult compound eye. (A) Wild type. (B) *ato$^{109\text{-}68}$*. (C) *ato$^{109\text{-}68}$/E(ato$^{109\text{-}68}$)4.12*. (D) *E(ato$^{109\text{-}68}$)4.12/E(ato$^{109\text{-}68}$)4.12*.

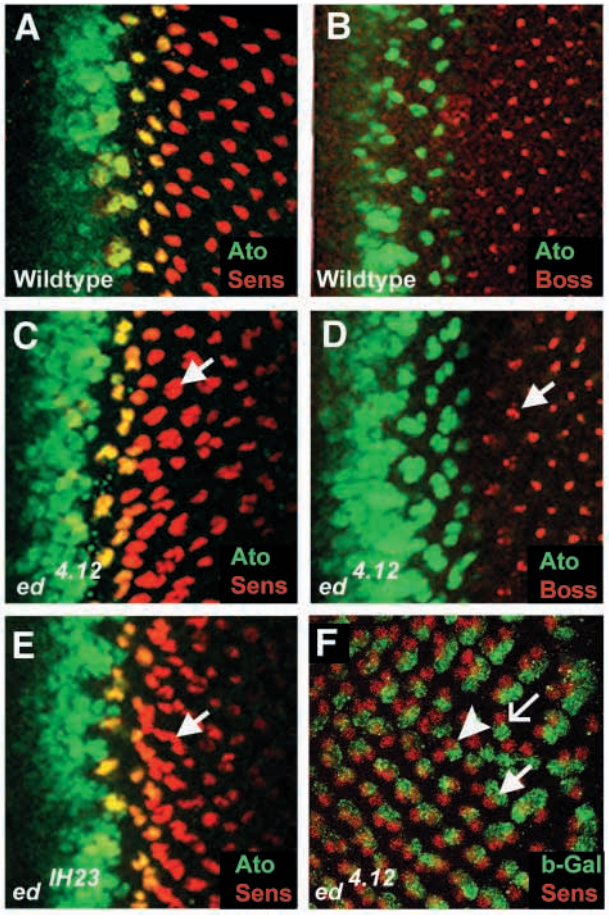

Fig. 2. R8 photoreceptors are frequently twinned in *ed* mutants. (A-E) Confocal microscopy for immunohistochemical detection of Ato (green) and Sens (red) (A,C,E), and Ato (green) and Boss (red) (B,D) in third larval instar eye discs. (A,B) Wild type. (C,D) *ed$^{4.12}$/ed$^{4.12}$*. (E) *ed^{lH23}/Df(2L)ed-dp*. A twinned R8 precursor pair is indicated by the arrow. (F) Expression of an R7 enhancer trap (R70-9) in an *ed$^{4.12}$* mutant background. Immunohistochemical detection of Sens (red) and β-galactosidase (green). The open arrow indicates a wild-type R8/7 pair. The closed arrow indicates twinned R8s with associated twinned R7s. The arrowhead indicates a twinned R8 with a single R7. Anterior is towards the left in all figures.

Table 1. *ed* mutations enhance the R8 twinning phenotype of $ato^{109\text{-}68}$

Genotype	Proportion of R8 positions with more than 1 R8 precursor	Mean number of R8s per position	Total number of R8 positions scored
$ato^{109\text{-}68}/+$	0.18±0.010	1.20±0.008	2627
$ato^{109\text{-}68}/ed^{4.12}$	0.32±0.011	1.35±0.01	1703
$ed^{4.12}/+$	0.0081±0.0021	1.01±0.002	1841

The larvae were raised at 29°C. Eye discs were stained with antibodies against Ato and Sens and the number of stained cells at each R8 position was scored. For each genotype five to nine eye discs were analysed.

interact with an *ato* loss-of-function mutant. For this purpose we used the ato^2 mutant, which has a severely reduced eye due to loss of an enhancer (White and Jarman, 2000). We found that ato^2 was suppressed by $ed^{4.12}$ (data not shown).

echinoid specifically affects R8 selection

Our results contrast with the report of Bai et al. (Bai et al., 2001), which stated that R8 formation is unaffected in the one allelic combination of *ed* that they examined. However, we find R8 twinning to be a consistent feature of all *ed* mutations that we have studied. This includes the strong EMS mutation ed^{lH23}, the P-element insertion *l(2)k01102* [also reported by Bai et al. (Bai et al., 2001)], which is an mRNA null (Spencer and Cagan, 2003), imprecise excision alleles of this P-element (E.L.R., N.M.W. and A.P.J., unpublished), and two newly generated EMS alleles, $ed^{4.4}$ and $ed^{6.1}$, the former of which is likely to be a null because of a nonsense mutation (Fig. 2E, Table 2). Interestingly, R8 twinning was most penetrant in the $ed^{4.12}$ allele, even though other alleles that are likely to be functional nulls, such as ed^{lH23}, *l(2)k01102* and $ed^{4.4}$, are more severe than $ed^{4.12}$ in terms of adult lethality. This would be consistent with *ed* having other functions elsewhere in development (Bai et al., 2001) (E.L.R., N.M.W. and A.P.J., unpublished).

Bai et al. (Bai et al., 2001) suggested that *ed* is an inhibitor of R7 photoreceptor recruitment because they observed extra R7 cells in *ed* mutant ommatidia. Downstream of R8 formation, we see variations in the number and arrangement of R7 and other photoreceptors in $ed^{4.12}$ eye sections (data not shown), which may result from recruitment defects but could also represent secondary effects of having supernumerary R8 cells. At least for $ed^{4.12}$, supernumerary R7 cells appear largely to be secondary, because an R7 enhancer trap line shows that the presence of extra R7s correlates very strongly with the presence of extra R8 cells. In an analysis of seven $ed^{4.12}$ eye discs, we found that 80% of twinned R8 cells were associated with twinned R7 cells (n=354), whereas we only observed a single example of twinned R7 cells associated with a single R8 cell (Fig. 2F).

ed is distinct from other mutations that cause R8 twinning

Mutation of *sca* or *ro* also results in an R8 twinning phenotype. *ro* is a negative regulator of *ato* that is expressed in cells that do not take on the R8 fate (Dokucu et al., 1996). Sca protein is normally secreted by the cells of the IG at a low level, and then from the selected R8 cell at a high level, probably preventing R8 twinning by interacting with the Notch receptor during lateral inhibition (Baker et al., 1990; Mlodzik et al., 1990; Powell et al., 2001). R8 twinning is not completely penetrant in *ro* or *sca* null mutants or in any of the *ed* mutants (Fig. 3A-C). Therefore none of these genes are absolutely required for R8 resolution. To test for redundancy, we analysed double mutants $ed^{4.12}$; ro^{X63} and $ed^{4.12}$ sca^{BP2}. These exhibit an increase in R8 twinning but in neither case is twinning fully penetrant (Fig. 3D,E; data not shown).

These data suggest that *ed*, *sca* and *ro* act independently and this is supported by differences in their phenotypes. *ro* mutants show a more general effect on *ato* expression than *ed*, with additional expression between the IGs (Fig. 3B). *sca* mutants differ from *ed* and *ro* in having a strong IG spacing defect in addition to R8 twinning (Fig. 3C). Moreover, R8 twinning in *ed* mutants is not the result of a general loss of *ro* or *sca* expression (Fig. 3F-I).

Egfr signalling is responsible for R8 twinning in *ed* mutants

R8 resolution requires communication within the equivalence group, and R8 twinning is therefore a failure in this communication. It might be presumed that R8 twinning results from a defect in Notch-mediated lateral inhibition, as is likely for *sca* (Powell et al., 2001). We did not find any evidence for this. The $ed^{4.12}$ R8 twinning phenotype is not altered by loss of one copy of the *Notch* null allele, N^{55e11} (Fig. 4A). Moreover

Table 2. R8 twinning is a consistent feature of *ed* mutants

Genotype	Proportion of R8 positions with more than1 R8 precursor	Mean number of R8s per position	Total number of R8 positions scored
Wild type	0	0	890
$ed^{4.12}/ed^{4.12}$	0.58±0.02	1.63±0.02	632
$ed^{4.12}/Df(2L)ed\text{-}dp$	0.54±0.015	1.60±0.02	1124
$ed^{lH23}/Df(2L)ed\text{-}dp$	0.47±0.017	1.51±0.02	855
$l(2)k01102/Df(2L)ed\text{-}dp$	0.30±0.012	1.08±0.01	1418
$ed^{4.4}/ed^{4.12}$	0.86±0.01	2.08±0.02	1234
$ed^{6.1}/ed^{4.12}$	0.73±0.012	1.83±0.02	1457

For each genotype five to nine eye discs were scored. The number of R8 precursors at each position was assessed by counting the numbers of Ato- or Sens-positive cells.

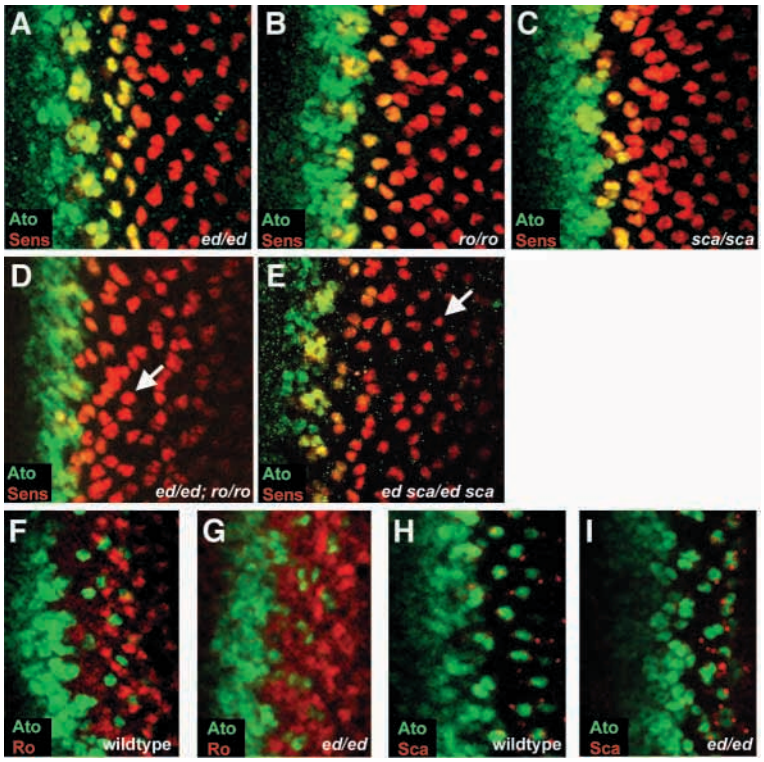

Fig. 3. *ed* is independent of the R8 twinning mutants *ro* and *sca*.
(A-I) Confocal microscopy of third larval instar eye imaginal discs.
(A-E) Immunohistochemical detection of Ato (green) and Sens (red).
(A) $ed^{4.12}/ed^{4.12}$. (B) ro^{X63}/ro^{X63}. (C) sca^{BP2}/sca^{BP2}. The phenotypes of the three mutants are distinct. (D) $ed^{4.12}/ed^{4.12};ro^{X63}/ro^{X63}$.
(E) $ed^{4.12},sca^{BP2}/ed^{4.12},sca^{BP2}$, twinning is not completely penetrant in D or E and arrows indicate single R8 cells. (F,G) Immunohistochemical detection of Ato (green) and Ro (red). (F) Wild type. (G) $ed^{4.12}/ed^{4.12}$, expression of Ato and Ro remains mutually exclusive in the *ed* mutant.
(H,I) Immunohistochemical detection of Ato (green) and Sca (red). (H) Wild type. (I) $ed^{4.12}/ed^{4.12}$, the additional R8 precursors express Sca.

we observed no change in expression in the morphogenetic furrow of the Notch target genes of the *E(spl)* complex, as detected by antibodies that recognise multiple family members (Ligoxygakis et al., 1998) (Fig. 5A,B) or by in situ hybridisation for *E(spl)m8* mRNA (data not shown). This suggests that Notch signalling is not the primary target of *ed*. In searching for other pathways that may be affected, we found that the R8 twinning phenotype of $ed^{4.12}$ is strongly suppressed by removing one copy of the *Egfr* gene ($Egfr^{IK35}$/+) (Fig. 4A-C) or of the *Ras1* gene (data not shown). Conversely, removing one copy of *argos*, which encodes an Egfr antagonist, strongly enhances the R8 twinning phenotype of $ed^{4.12}$ (Fig. 4A). This is particularly striking because null mutations of *argos* exhibit no R8 twinning phenotype (Baonza et al., 2001; Yang and Baker, 2001). These data suggest that *ed* may encode an Egfr antagonist that functions during R8 specification.

These interactions suggest that derepression of Egfr signalling may be the underlying cause of R8 twinning in *ed* mutants. This is unexpected as Egfr signalling is not required for wild-type R8 specification. To test if Egfr signalling is required for R8 twinning, we created *Egfr*-null ($Egfr^{IK35}$) clones in an $ed^{4.12}$ homozygous background. We found that although R8 spacing is abnormal in such clones, R8s rarely appeared twinned, demonstrating that the absence of Egfr signalling can fully rescue the $ed^{4.12}$ R8 twinning phenotype (Fig. 4A,D,E). A few cases of apparent R8 twins were observed in such clones but their nuclei were always in different focal planes of the epithelium, unlike the apically positioned nuclei of twinned R8 cells in *ed* and other mutants. We conclude that these are probably not R8 twins *sensu stricto* but may instead reflect the patterning disruption seen in $Egfr^{IK35}$ clones. One potential explanation for Egfr dependence of the *ed* phenotype is that twinned R8s result from mis-fated R2,5 photoreceptors rather than from cell interaction problems within the R8 equivalence group. As Egfr is required for R1-7 recruitment, such cells would therefore be missing in $Egfr^{IK35}$ clones, thereby secondarily rescuing the *ed* phenotype. To test this, we looked at the requirement for the Egfr ligand encoded by *spitz* (*spi*). R1-7 recruitment requires *spi* (Tio et al., 1994), whereas earlier Egfr functions are thought to require the related *spi-2* or *keren* gene (Baonza et al., 2001). Unlike $Egfr^{IK35}$ clones, we found that R8 twinning of $ed^{4.12}$ is not affected in *spi*-null clones (Fig. 4A,F). Therefore, twinning is not a defective outcome of the normal Egfr-dependent photoreceptor recruitment process. It suggests that twinning occurs during R8 equivalence group resolution via a novel Egfr-dependent mechanism.

In contrast to *ed*, R8 twinning in *sca* mutants is apparently not caused by Egfr derepression. Examining R8 twinning in $Egfr^{IK35}$ *sca* double mutant clones is difficult because of their combined IG spacing defects (Baonza et al., 2001). However, we can unambiguously observe twinned R8s in such clones (Fig. 4G). Given the strong link between *sca* and the Notch signalling pathway (Baker and Zitron, 1995; Powell et al., 2001), it is likely that R8 twinning in *sca* mutants is mediated by disruption of Notch signalling. This finding reinforces the significance and specificity of Egfr involvement in the *ed* twinning phenotype. It also demonstrates that R8 twinning can be caused by at least two different mechanisms, which are differentially affected in *ed* and *sca* mutants. This would explain the lack of strong interactions between *ed* and *sca*.

Egfr signalling is hyperactivated in *ed* mutants

Our data indicate that Egfr inhibition by *ed* is required for correct R8 resolution. To see how Egfr signalling may be affected by *ed*, we examined the expression of *pointed-P1* (*pnt-P1*) mRNA and of the phosphorylated form of the Erk MAP kinase (dpErk) (Gabay et al., 1996; Gabay et al., 1997). The pattern and level of each reflects a direct response to Egfr activation. Interestingly, in wild-type eye discs, dpErk (Kumar et al., 1998; Wasserman et al., 2000) and *pnt-P1* mRNA are both detectable in the IGs and R8 equivalence groups, indicating that Egfr signalling is active in these locations (Fig. 5C,E). Clearly, such signalling does not normally interfere with R8 equivalence group resolution; it may mediate a proposed function of Egfr signalling during IG spacing (Dominguez et al., 1998; Spencer et al., 1998; Chen and Chien, 1999; Lesokhin et al., 1999; Yang and Baker, 2001). In *ed* mutant eye discs, the patterns of *pnt-P1* and dpErk are unchanged, but the

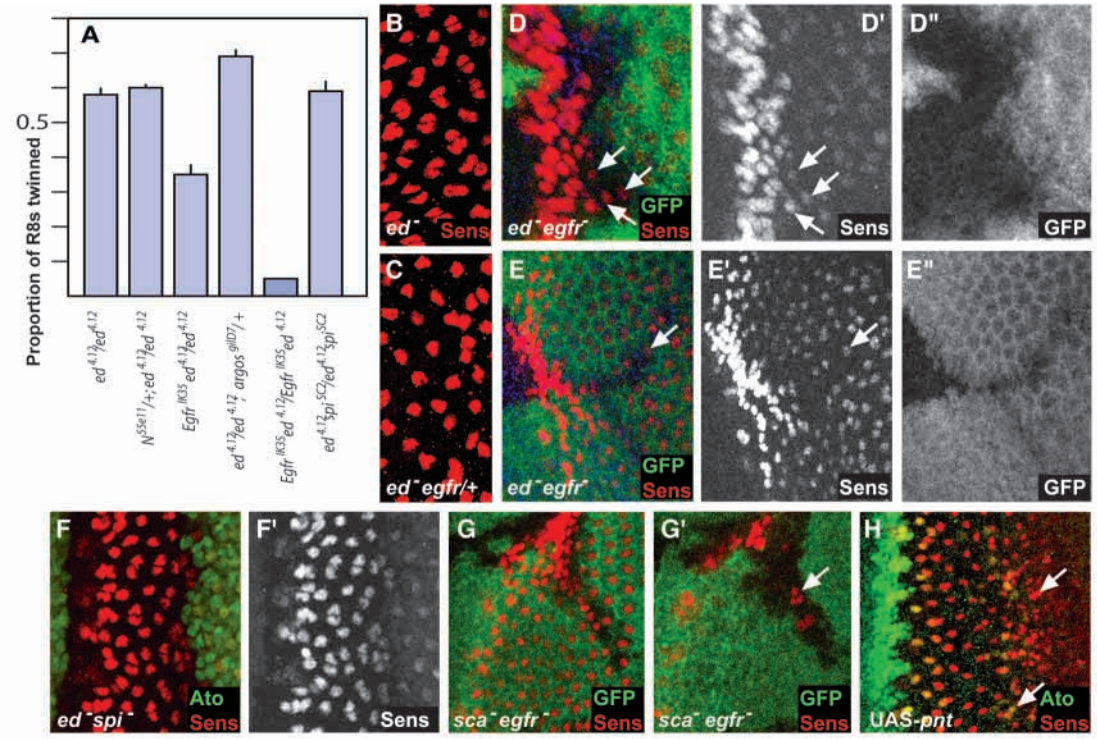

Fig. 4. Egfr signalling is responsible for R8 twinning in $ed^{4.12}$. (A) Graph to show the interactions between $ed^{4.12}$ and the Egfr pathway. Genotype is plotted against the proportion of equivalence groups not resolving to single R8 cells. The line above each bar represents the standard error of the mean. Six to nine eye discs were counted of each genotype. (B-H) Confocal microscopy of third larval instar eye imaginal discs. (B,C) Suppression of R8 twinning (Sens expression) by $Egfr^{IK35}$. (B) Homozygous *ed* ($ed^{4.12}/ed^{4.12}$). (C) Homozygous *ed* with loss of one copy of *Egfr* ($ed^{4.12}$ $Egfr^{IK35}/ed^{4.12}$ +). (D-E″) Loss of R8 twinning in *Egfr* clones. (D,E) $Egfr^{IK35}$ homozygous clones in an $ed^{4.12}/ed^{4.12}$ background. Immunohistochemical detection of Sens (red, D,D′,E,E″), β-galactosidase (green, D,D″,E,E″) and DAPI (blue). The absence of the green β-galactosidase staining marks the *Egfr* homozygous clone. Arrows indicate single R8 cells within the clone. (F,F′) spi^{SC2} clone in an $ed^{4.12}/ed^{4.12}$ background. Immunohistochemical detection of Sens (red) and nlsGFP (green). The absence of the nlsGFP marks the *spi*-null region, twinned R8 precursors can be seen in both the presence and absence of *spi*. (G,G′) $Egfr^{IK35}$ clone in an sca^{BP2}/sca^{BP2} background. Immunohistochemical detection of Sens (red) and β-galactosidase (green). The absence of the green β-galactosidase staining indicates the *sca Egfr* double homozygous clone (the rest of the disc is heterozygous for *sca* and *Egfr* and so displays no R8 phenotype). G is a more basal section than G′, twins and triplets of R8s can readily be seen in the more apical sections of the clone (arrow). (H) Overexpression of *pnt-P1* posterior to the morphogenetic furrow (genotype *GMR-Gal4/UAS-pntP1*). Immunohistochemical detection of Sens (red) and Ato (green) reveals twinned cells with R8 characteristics (arrows).

levels of both are elevated in the IGs and equivalence groups (Fig. 5D,F). Of the *ed* mutations analysed ($ed^{4.12}$, $ed^{lH23}/Df(2L)ed\text{-}dp$, and $l(2)k01102/Df(2L)ed\text{-}dp$), this effect is most noticeable for $ed^{4.12}$, thereby correlating with the higher incidence of R8 twinning observed for this allele. This suggests that *ed* inhibits the level of Egfr signalling rather than the pattern, and that this is normally sufficient to prevent such signalling from interfering with R8 resolution. It also suggests that *ed* antagonises Egfr signalling upstream of Erk activation.

Given these findings, we asked whether experimental Egfr pathway activation might mimic *ed* mutation and provoke R8 fates. Interestingly, we found evidence that this is the case if we drive expression of downstream components of the pathway. Thus, when UAS-*pnt-P1* or UAS-Raf^{Act} was expressed in the eye posterior to the morphogenetic furrow using a GMR-Gal4 driver, we could detect frequent instances of twinned *sens*-expressing cells. Some of these twins co-express *ato*, although more posteriorly than normal (Fig. 4H, and data not shown). These data suggest that the inhibitory function of *ed* can be bypassed by expression of these components, implying that *ed* functions upstream of *Raf*. This twinning phenotype, however, could not be reproduced by identical misexpression of UAS-*sSpi*, the activated form of the Spi ligand (data not shown). We showed earlier that Spi is not the ligand responsible for R8 twinning, but if we assume that UAS-*sSpi* is otherwise able to act in this situation as it can in other Egfr-mediated processes in the eye (Freeman, 1996), then these data suggest that *ed* cannot be bypassed by increased ligand and that *ed* therefore acts downstream of ligand function. These findings, and the membrane associated nature of the Ed protein, support a model in which Ed interacts directly with Egfr or a closely associated component. Consistent with this, Ed protein is found at the apical cell surface with Egfr (E.L.R., N.M.W. and A.P.J., unpublished).

ed is required within the equivalence group to prevent R8 twinning

Clonal analysis was used to explore whether *ed* prevents Egfr signalling to prospective R8 cells or prevents R8 cells from receiving or responding to the signal. We generated ed^{lH23},

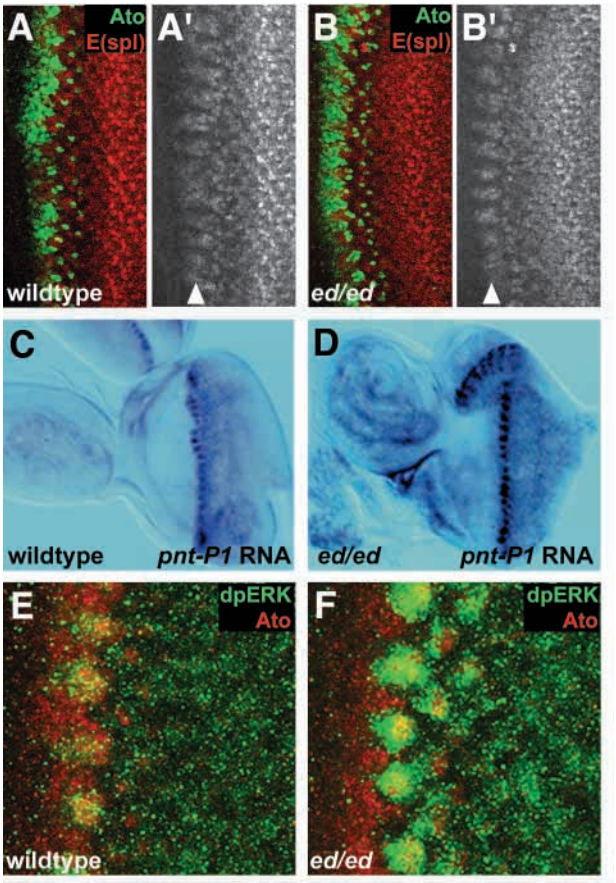

Fig. 5. Levels of Egfr signalling are increased in *ed* mutants. (A-B′) Confocal microscopy for immunohistochemical detection of Ato (green) and mAb323, which detects multiple E(spl) proteins (red), in third larval instar eye discs. (A,A′) Wild type. (B,B′) $ed^{4.12}/ed^{4.12}$. Levels of E(spl) are not altered in the mutant morphogenetic furrow (arrowhead). (C,D) Light microscope images of *pnt-P1* mRNA in third larval instar eye discs. (C) Wild type, showing expression in the IGs. (D) $ed^{4.12}/ed^{4.12}$. *pnt-P1* expression is greater in D. (E,F) Confocal microscopy for immunohistochemical detection of dp-Erk (green) and Ato (red) in third larval instar eye imaginal discs. (E) Wild type, showing expression in the IGs. (F) $ed^{4.12}/ed^{4.12}$. Levels of dpErk are higher in F.

$ed^{6.1}$ and $ed^{4.4}$ mutant clones in eye discs and examined them for Ato, Sens and Boss expression. Where wild-type and mutant tissue was juxtaposed, R8 twins could frequently straddle the border, being composed of one wild-type and one mutant R8 cell (Fig. 6A, arrow). These presumably represent cases where an equivalence group was bisected by the clone border, and are consistent with *ed* acting both autonomously and non-autonomously. We also observed rare cases of R8 twins consisting of two genetically wild-type cells immediately juxtaposed to mutant tissue (five cases out of 45 clones examined) (Fig. 6B, arrowhead). No R8 twins consisting of wild-type cells were ever observed elsewhere in these discs. This can be explained if the third member of an equivalence group was mutant for *ed* but did not differentiate as an R8, therefore suggesting that *ed* acts non-autonomously in this case. Moreover, we suggest that the low frequency of this class of twins implies that the *ed*-associated signalling events are occurring within the equivalence group rather than between the equivalence group and surrounding cells. In other words, the phenotype is only seen on the rare occasions when an equivalence group is bisected by the clone but the mutant cell does not become an R8.

DISCUSSION

During eye development, *ed* is an Egfr antagonist that inhibits Egfr protein itself or a closely associated component of the signalling pathway. The Egfr signalling pathway functions in diverse inductive events during development. Clearly such a commonly deployed pathway must be tightly regulated to prevent inappropriate inductive events occurring at other times and locations. Our analysis of *ed* suggests that it is a mediator of such regulation. Although Egfr signalling is not required directly for wild-type R8 fate specification, derepressed signalling in *ed* mutants induces multiple R8 cells (the R8 twinning phenotype). *ed* is notable, therefore, because its mutation exposes a new and unexpected outcome of signalling (R8 specification), rather than expansion of an existing Egfr function.

The finding that Egfr signalling *can* induce R8 specification even though it does not normally do so may resolve the contradictory evidence for Egfr function in R8 specification. Recent studies definitively

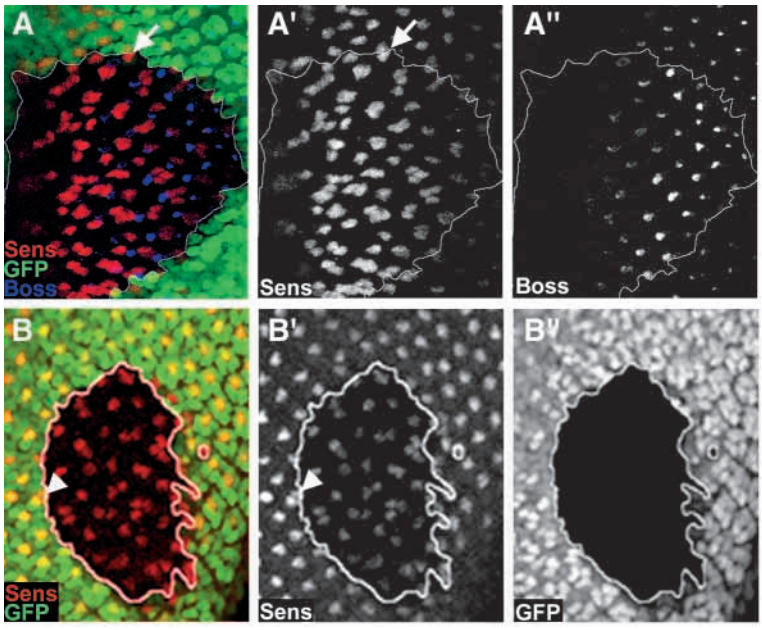

Fig. 6. *ed* is required in the R8 equivalence group to prevent R8 twinning. Mosaic analysis of *ed* alleles examined by confocal microscopy for immunohistochemical detection of Sens (red), Boss (blue) and nlsGFP (green) in third larval instar eye imaginal discs. The mosaic clone is distinguished by the absence of nlsGFP and the border has been marked with a white line. (A) $ed^{6.1}$ homozygous clone. (A) Overlay. (A′) Red channel. (A″) Blue channel. A mixed twin of a mutant and a wild-type R8 at the clone border has been marked by an arrow. (B) $ed^{4.4}$ homozygous clone. (B) Overlay. (B′) Red channel. (B″) Green channel. An R8 twin consisting of two wild-type cells at the clone border is marked with an arrowhead.

show that R8 cells can be specified in the absence of Egfr, albeit aberrantly (Baonza et al., 2001; Kumar et al., 1998; Yang and Baker, 2001). Yet Spencer et al. (Spencer et al., 1998) presented data that strongly suggested a link between R8 selection (not just IG spacing) and Egfr/Ras signalling. They observed that expression of activated Ras results in strong *ato* upregulation and ectopic R8 cells and that *argos* misexpression inhibits R8 formation (Spencer et al., 1998). The latter findings may allude not to an Egfr requirement during R8 selection, but to the ability of aberrant Egfr signalling to induce R8s.

Bai et al. (Bai et al., 2001) suggested that *ed* acts downstream of the Egfr target gene *pnt-P1* in R7 specification and based on this they proposed a hypothetical parallel signalling pathway that antagonises Egfr. Our observations are more consistent with membrane-associated Ed interacting directly with Egfr or with immediate downstream components. We observed increased activated MAPK and *pnt-P1* expression in *ed* mutants, which suggests that *ed* acts upstream of MAPK activation in the Egfr signalling pathway. Moreover, forced expression of *pnt-P1* or activated *Raf* can bypass the inhibitory function of *ed*, whereas *spi* cannot. This is entirely consistent with the finding that Ed is colocalised with Egfr at the cell surface (E.L.R., N.M.W. and A.P.J., unpublished) and that Ed can bind Egfr protein and is phosphorylated in response to Egfr activation (Spencer and Cagan, 2003). Moreover, these findings are consistent with known features of the L1 family of cell adhesion molecules (CAMs), with which Ed protein shares extensive homology in its extracellular portion (Bai et al., 2001). L1 CAMs are involved in the control of axon outgrowth, where they are associated with regulation of Fgfr and Egfr activity (Williams et al., 1994; Schaefer et al., 1999; Kamiguchi and Lemmon, 2000; Garcia-Alonso et al., 2000). In brain extracts, L1 physically associates with the MAPK cascade components Raf1 and Erk2, while in vitro Erk2 can phosphorylate the L1 cytoplasmic domain (Schaefer et al., 1999). Interestingly, our clonal analysis suggests both autonomy and nonautonomy, suggesting that Ed might be able to interact with Egfr in trans as well as in cis. If so, this might imply an association between the extracellular domains of the two proteins. The molecular mechanism of L1 function is unclear, although its endocytosis may be important for downstream events (Schmid et al., 2000). This may have implications for Ed function. However, the intracellular domain of Ed is distinct from that of L1 and there is evidence that tyrosine phosphorylation within this domain is important for function, and that Ed may act on Egfr via an interaction with the phosphatase encoded by *corkscrew* (Spencer and Cagan, 2003).

Unlike negative regulators such as *argos*, mutation of *ed* does not alter the pattern of Egfr activation, just the intensity, suggesting that the function of *ed* is to limit the level or duration of activation. In support of this, Spencer and Cagan (Spencer and Cagan, 2003) provide biochemical evidence that the inhibitory activity of Ed is dependent post-translationally on Egfr signalling, thereby providing a negative feedback mechanism to damp down Egfr signalling. *ed* does not completely suppress Egfr signalling around the morphogenetic furrow, presumably because such signalling has some role to play. Indeed this wild-type level of signalling may be important for mediating the proposed inhibitory Egfr/Ras/Raf process in which one row of IGs helps to pattern the next row (Chen and Chien, 1999; Baonza et al., 2001; Yang and Baker, 2001) (Fig. 7). Such activity occurs at the same time that R8 fate must be restricted within the IGs by lateral inhibition. Given the inductive nature of Egfr signalling generally, such signalling could therefore interfere with R8 resolution. Therefore, in R8 proneural clusters *ed* must suppress a potential outcome of Egfr signalling in the morphogenetic furrow (induction of R8 fate) rather than the signalling itself.

Ed protein at the cell surface (E.L.R., N.M.W. and A.P.J., unpublished) may provide a contact mechanism that preferentially inhibits short range R8 inductive signalling rather than long-range signalling in which the diffusible antagonist Argos may participate (Baonza et al., 2001; Yang and Baker, 2001). This may explain why simply increasing EGF receptor activity does not normally cause R8 twinning. For example, mutations of other negative regulators of Egfr (*argos*, *sprouty*, *kekkon I*) do not show R8 twinning, despite raising levels of Egfr signalling (Casci et al., 1999; Ghiglione et al., 1999; Baonza et al., 2001; Yang and Baker, 2001). Neither does increased expression of Spi ligand (this paper). The wild-type function of *ed* must be sufficient to quash any level of Egfr signalling specifically in the context of R8 selection.

Why does Egfr signalling induce R8 fate in *ed* mutants? It may reflect the general inductive ability of Egfr in the context of cells primed to become R8s. An alternative, however, is

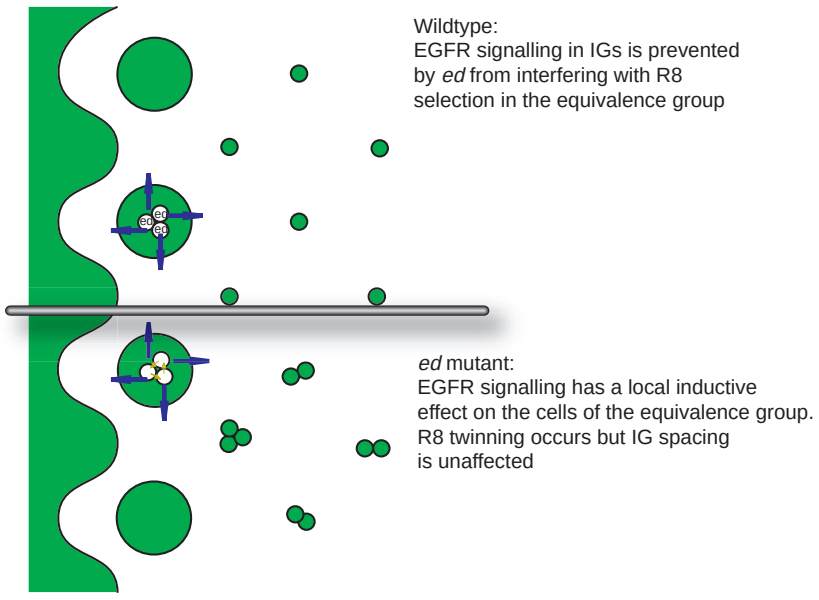

Fig. 7. Schematic representing the Egfr-mediated signalling events during Ato expression (green). In wild type, Egfr signalling is occurring in the IGs. This signalling occurs at the same time as R8 precursor selection within the equivalence group, and the role of Ed is to prevent the Egfr signalling from interfering with this process. In *ed* mutants, there is no Ed protein and Egfr signalling has a local inductive effect on the cells of the equivalence group resulting in the selection of more than one R8 precursor.

suggested by the close relationship between Egfr and *ato* function. The wild-type level of Egfr signalling in the morphogenetic furrow is dependent on *ato* (Chen and Chien, 1999). Moreover, increased *ato* expression in R8 precursors can provoke R8 twinning in a non-autonomous manner (White and Jarman, 2000), presumably by hyperactivation of Egfr signalling. This relationship between *ato* and Egfr is reminiscent of the normal function of *ato* during chordotonal SOP selection. In the femoral chordotonal organ, *ato* triggers SOP recruitment by activating Egfr signalling (zur Lage and Jarman, 1999). In turn, Egfr signalling activates *ato* and SOP fate in uncommitted cells in a manner that is suggestive of the aberrant effect of Egfr on R8 specification in *ed* mutants. We speculate therefore that R8 twinning might be an aberrant outcome of an *ato*-Egfr neural recruitment network in the wrong time and place. It is notable that chordotonal recruitment is unaffected in *ed* mutants (E.L.R., N.M.W. and A.P.J., unpublished). Thus, by modulating Egfr signalling specifically in the eye, *ed* enables the *ato*-Egfr network to be customised to the specific needs of R8 precursor patterning, where Egfr signalling must be activated by *ato* but supernumerary R8 specification must be prevented (Fig. 7). A key principle of development is the continual redeployment of a handful of intercellular signalling pathways such as Egfr. As such, much of development must involve similar instances of suppression of potential developmental outcomes that would result from the re-use of signalling networks.

We thank Bridget Lovegrove and Iain Chalmers for their contributions to this work, and Antonio Baonza for much advice. We greatly appreciate Susan Spencer and Ross Cagan for their discussions and communication of unpublished results. The following are thanked for reagents: Jui-Chou Hsu, Nick Baker, Matthew Freeman, Antonio Baonza, Marla Sokolowski, Sarah Bray, Hugo Bellen and Barry Dickson. This work was supported by a Wellcome Trust Prize studentship (E.L.R.). A.P.J. is a Wellcome Trust Senior Research Fellow.

REFERENCES

Bai, J., Chiu, W., Wang, J., Tzeng, T., Perrimon, N. and Hsu, J. (2001). The cell adhesion molecule Echinoid defines a new pathway that antagonizes the *Drosophila* EGF receptor signaling pathway. *Development* **128**, 591-601.

Baker, N. E., Mlodzik, M. and Rubin, G. M. (1990). Spacing differentiation in the developing *Drosophila* eye – a fibrinogen-related lateral inhibitor encoded by *scabrous*. *Science* **250**, 1370-1377.

Baker, N. E., Yu, S. and Han, D. (1996). Evolution of proneural Atonal expression during distinct regulatory phases in the developing *Drosophila* eye. *Curr. Biol.* **6**, 1290-1301.

Baker, N. E. and Zitron, A. E. (1995). *Drosophila* eye development: *Notch* and *Delta* amplify a neurogenic pattern conferred on the morphogenetic furrow by *scabrous*. *Mech. Dev.* **49**, 173-189.

Baonza, A., Casci, T. and Freeman, M. (2001). A primary role for the epidermal growth factor receptor in ommatidial spacing in the *Drosophila* eye. *Curr. Biol*. **11**, 396-404.

Casci, T., Vinos, J. and Freeman, M. (1999). Sprouty, an intracellular inhibitor of Ras signaling. *Cell* **96**, 655-665.

Chen, C.-K. and Chien, C.-T. (1999). Negative regulation of *atonal* in proneural cluster formation of *Drosophila* R8 photoreceptors. *Proc. Natl Acad. Sci. USA* **96**, 5055-5060.

de Belle, J. S., Sokolowski, M. B. and Hilliker, A. J. (1993). Genetic analysis of the *foraging* microregion of *Drosophila melanogaster*. *Genome* **36**, 94-101.

Dokucu, M. E., Zipursky, S. L. and Cagan, R. L. (1996). *atonal*, *rough* and the resolution of proneural clusters in the developing *Drosophila* retina. *Development* **122**, 4139-4147.

Dominguez, M., Wasserman, J. D. and Freeman, M. (1998). Multiple functions of the EGF receptor in *Drosophila* eye development. *Curr. Biol.* **8**, 1039-1048.

Ellis, M. C., Weber, U., Wiersdorff, V. and Mlodzik, M. (1994). Confrontation of *scabrous* expressing and non-expressing cells is essential for normal ommatidial spacing in the *Drosophila* eye. *Development* **120**, 1959-1969.

Frankfort, B. J., Nolo, R., Zhang, Z., Bellen, H. and Mardon, G. (2001). senseless repression of *rough* Is required for R8 photoreceptor differentiation in the developing *Drosophila* eye. *Neuron* **32**, 403-414.

Freeman, M. (1996). Reiterative use of the EGF receptor triggers differentiation of all cell types in the *Drosophila* eye. *Cell* **87**, 651-660.

Freeman, M., Klämbt, C., Goodman, C. S. and Rubin, G. M. (1992). The *argos* gene encodes a diffusible factor that regulates cell fate decisions in the *Drosophila* eye. *Cell* **69**, 963-975.

Gabay, L., Scholz, H., Golembo, M., Klaes, A., Shilo, B. Z. and Klambt, C. (1996). EGF receptor signaling induces *pointed P1* transcription and inactivates Yan protein in the *Drosophila* embryonic ventral ectoderm. *Development* **122**, 3355-3362.

Gabay, L., Seger, R. and Shilo, B. Z. (1997). In situ activation pattern of *Drosophila* EGF receptor pathway during development. *Science* **277**, 1103-1106.

Garcia-Alonso, L., Romani, S. and Jimenez, F. (2000). The EGF and FGF receptors mediate neuroglian function to control growth cone decisions during sensory axon guidance in *Drosophila*. *Neuron* **28**, 741-752.

Ghiglione, C., Carraway, K. L., 3rd, Amundadottir, L. T., Boswell, R. E., Perrimon, N. and Duffy, J. B. (1999). The transmembrane molecule kekkon 1 acts in a feedback loop to negatively regulate the activity of the *Drosophila* EGF receptor during oogenesis. *Cell* **96**, 847-856.

Heberlein, U. and Rubin, G. M. (1991). *Star* is required in a subset of photoreceptor cells In the developing *Drosophila* retina and displays dosage sensitive interactions with rough. *Dev. Biol.* **144**, 353-361.

Jarman, A. P., Grell, E. H., Ackerman, L., Jan, L. Y. and Jan, Y. N. (1994). *atonal* is the proneural gene for *Drosophila* photoreceptors. *Nature* **369**, 398-400.

Jarman, A. P., Sun, Y., Jan, L. Y. and Jan, Y. N. (1995). Role of the proneural gene, *atonal*, in formation of *Drosophila* chordotonal organs and photoreceptors. *Development* **121**, 2019-2030.

Kamiguchi, H. and Lemmon, V. (2000). IgCAMs: bidirectional signals underlying neurite growth. *Curr Opin Cell Biol* **12**, 598-605.

Klaes, A., Menne, T., Stollewerk, A., Scholz, H. and Klambt, C. (1994). The Ets transcription factors encoded by the *Drosophila* gene *pointed* direct glial cell differentiation in the embryonic CNS. *Cell* **15**, 149-160.

Kumar, J. P., Tio, M., Hsiung, F., Akopyan, S., Gabay, L., Seger, R., Shilo, B. Z. and Moses, K. (1998). Dissecting the roles of the *Drosophila* EGF receptor in eye development and MAP kinase activation. *Development* **125**, 3875-3885.

Lesokhin, A. M., Yu, S. Y., Katz, J. and Baker, N. E. (1999). Several levels of EGF receptor signaling during photoreceptor specification in wild-type, *Ellipse*, and null mutant *Drosophila*. *Dev. Biol.* **205**, 129-144.

Ligoxygakis, P., Yu, S.-Y., Delidakis, C. and Baker, N. E. (1998). A subset of *Notch* functions during *Drosophila* eye development require *Su(H)* and the *E(spl)* complex. *Development* **125**, 2893-2900.

Lindsley, D. L. and Zimm, G. G. (1992). *The Genome of* Drosophila melanogaster. San Diego: Academic Press.

Mlodzik, M., Baker, N. E. and Rubin, G. M. (1990). Isolation and expression of *scabrous*, a gene regulating neurogenesis in *Drosophila*. *Genes Dev.* **4**, 1848-1861.

Newsome, T. P., Asling, B. and Dickson, B. J. (2000). Analysis of Drosophila photoreceptor axon guidance in eye-specific mosaics. *Development* **127**, 851-860.

Powell, P. A., Wesley, C., Spencer, S. and Cagan, R. L. (2001). Scabrous complexes with Notch to mediate boundary formation. *Nature* **409**, 626-630.

Schaefer, A. W., Kamiguchi, H., Wong, E. V., Beach, C. M., Landreth, G. and Lemmon, V. (1999). Activation of the MAPK signal cascade by the neural cell adhesion molecule L1 requires L1 internalization. *J. Biol. Chem.* **274**, 37965-37973.

Schmid, R.-S., Pruitt, W. M. and Maness, P. F. (2000). A MAP kinase-signalling pathway mediates neurite outgrowth on L1 and requires Src-dependent endocytosis. *J. Neurosci*. **20**, 4177-4188.

Scholz, H., Sadlowski, E., Klaes, A. and Klambt, C. (1997). Control of

midline glia development in the embryonic *Drosophila* CNS. *Mech. Dev.* **64**, 137-151.

Spencer, S. and Cagan, R. (2003). Echinoid is essential for regulation of EGFR signaling and R8 formation during Drosophila eye development. *Development* **130**, 3725-3733.

Spencer, S., Powell, P., Miller, D. and Cagan, R. (1998). Regulation of EGF receptor signaling establishes pattern across the developing *Drosophila* retina. *Development* **125**, 4777-4790.

Tio, M., Ma, C. and Moses, K. (1994). *spitz*, a *Drosophila* homolog of transforming growth factor-α, is required in the founding photoreceptor cells of the compound eye facets. *Mech. Dev.* **48**, 13-23.

Van Vactor, D. L., Cagan, R. L., Kramer, H. and Zipursky, S. L. (1991). Induction in the developing compound eye of *Drosophila* – multiple mechanisms restrict R7 induction to a single retinal precursor cell. *Cell* **67**, 1145-1155.

Wasserman, J. D., Urban, S. and Freeman, M. (2000). A family of *rhomboid*-like genes: Drosophila *rhomboid-1* and *roughoid/rhomboid-3* cooperate to activate EGF-receptor signaling. *Genes Dev.* **14**, 1651-1663.

White, N. M. and Jarman, A. P. (2000). *Drosophila atonal* controls photoreceptor R8-specific properties and modulates both receptor tyrosine kinase and Hedgehog signalling. *Development* **127**, 1681-1689.

Williams, E. J., Furness, J., Walsh, F. S. and Doherty, P. (1994). Activation of the FGF receptor underlies neurite outgrowth stimulated by L1, N-CAM, and N-cadherin. *Neuron* **13**, 583-594.

Xu, T. and Rubin, G. M. (1993). Analysis of genetic mosaics in developing and adult *Drosophila* tissues. *Development* **117**, 1223-1237.

Yang, L. and Baker, N. E. (2001). Role of the EGFR/Ras/Raf pathway in specification of photoreceptor cells in the *Drosophila* retina. *Development* **128**, 1183-1191.

zur Lage, P. and Jarman, A. P. (1999). Antagonism of EGFR and Notch signalling in the reiterative recruitment of *Drosophila* adult chordotonal sense organ precursors. *Development* **126**, 3149-3157.